**Supplementary Information**

# Ultraefficient Piezocatalyst of Surface Functionalized $Ti_3C_2T_x$ MXene: Synchronous Hydrogen Evolution and Wastewater Treatments

Sz-Nian Lai[1, 2], Winston Yenyu Chen[5], Chao-Chun Yen[6], Yin-Song Liao[1,4], Po-Han Chen[1], Lia Stanciu[5] and Jyh Ming Wu[1, 3*]

[1]Department of Materials Science and Engineering, National Tsing Hua University, 101, Section 2 Kuang Fu Road, Hsinchu 300, Taiwan.

[2]Ph.D. Program in Prospective Functional Materials Industry, National Tsing Hua University, 101, Section 2 Kuang Fu Road, Hsinchu 300, Taiwan.

[3]High Entropy Materials Center, National Tsing Hua University, 101, Section 2 Kuang Fu Road, Hsinchu 300, Taiwan.

[4]Tsing Hua Interdisciplinary Program, National Tsing Hua University, 101, Section 2 Kuang Fu Road, Hsinchu 300, Taiwan.

[5]School of Materials Engineering, Purdue University, West Lafayette, IN 47907, USA.

[6]Department of Materials Science and Engineering, National Chung Hsing University, 145, Xingda Road, Taichung 402, Taiwan.

* Prof. J. M. Wu, Email:wujm@mx.nthu.edu.tw

**Supplementary Information of S1**

Figure S1 compares the piezodegradation performance of $Ti_3C_2T_x$-FOTS for different RB concentrations (10–30 ppm). The results indicate that higher dye concentrations necessitate a prolonged duration to complete the degradation of RB molecules. However, the $Ti_3C_2T_x$-FOTS still can reach 100% decomposition of dye molecules for 30 ppm concentration in one hour, showing its high piezodegradation activity.

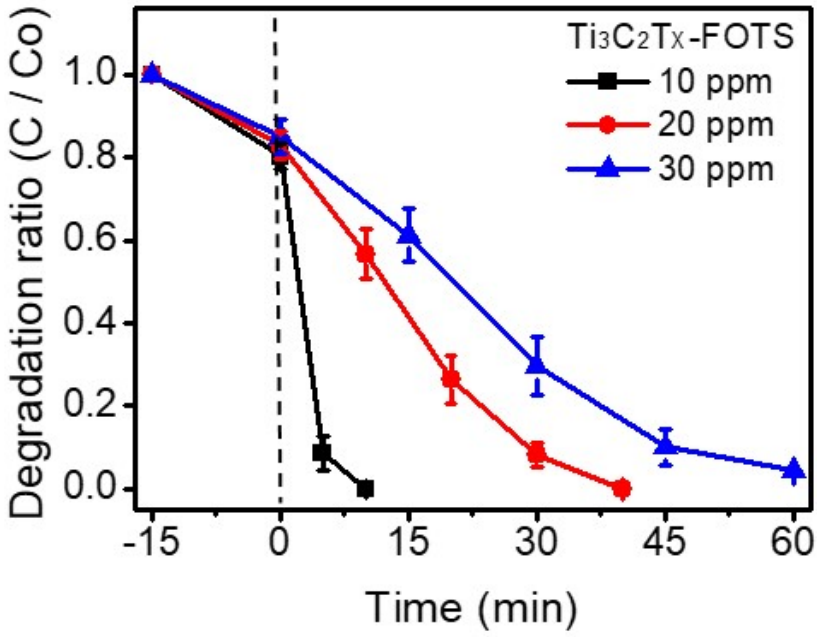


Figure S1. The degradation performance of $Ti_3C_2T_x$-FOTS at various initial concentrations of RB.

The intensity of Ti-O bonding for $Ti_3C_2T_x$, $Ti_3C_2T_x$-CPTMS, and $Ti_3C_2T_x$-FOTS after the degradation reaction. Figure S1a shows the $Ti_3C_2T_x$ without SAMs, which has a high intensity of oxidation after the degradation reaction. Figures S1b-c show the results of $Ti_3C_2T_x$-CPTMS and $Ti_3C_2T_x$-FOTS, proving that SAMs act as a protective

layer to improve the antioxidation properties. Figure S1d further shows the calculated area ratio for Ti–O peak to quantify the antioxidation activity of $Ti_3C_2T_x$, $Ti_3C_2T_x$-CPTMS, and $Ti_3C_2T_x$-FOTS, indicating that $Ti_3C_2T_x$-FOTS exhibited the best antioxidant activity.

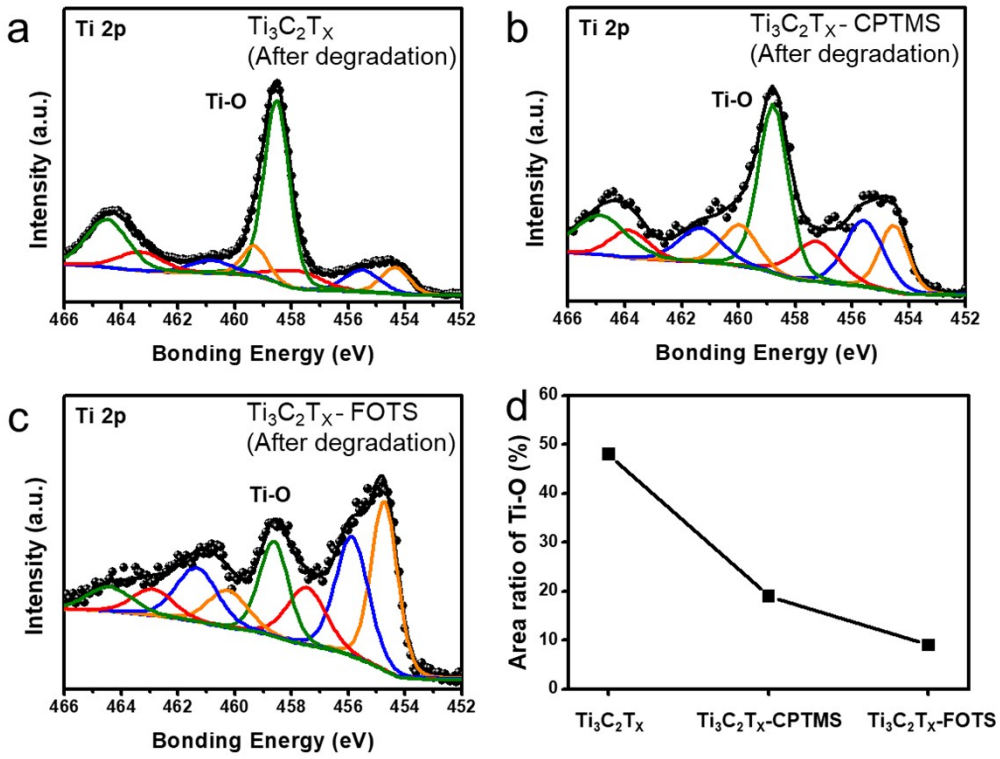


Figure S2. High-resolution XPS spectra of (a)-(c) Ti 2p of $Ti_3C_2T_x$, $Ti_3C_2T_x$-CPTMS, and $Ti_3C_2T_x$-FOTS confirming the antioxidation ability of SAMs after the dye degradation reaction. (d) The calculated area ratio of Ti–O peak is fitted from Ti 2P spectra for $Ti_3C_2T_x$, $Ti_3C_2T_x$ -CPTMS, and $Ti_3C_2T_x$ -FOTS.

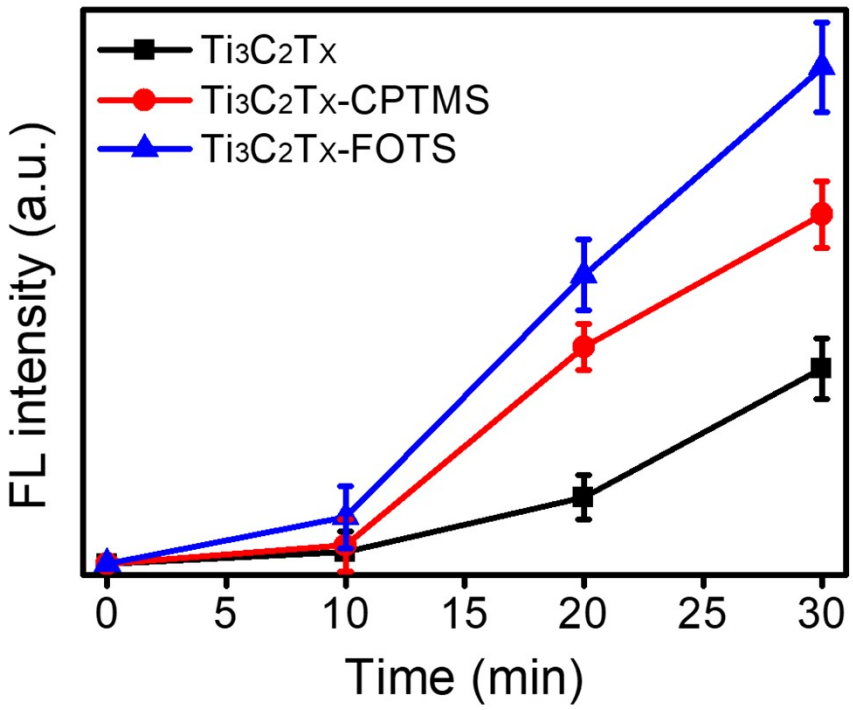


Figure S3. FL analysis results of $Ti_3C_2T_x$, $Ti_3C_2T_x$-CPTMS, and $Ti_3C_2T_x$-FOTS under ultrasonic vibration.

**Supplementary Information of S2**

To investigate whether the RB dye molecules were physically adsorbed on the catalyst surface during the degradation process, XPS was used to analyze N 1s bonding on the pure RB dye and the degraded catalyst. The chemical formula of RB dye is $C_{28}H_{31}ClN_2O_3$, which can produce the by-products of $CO_2$, $NH_4^+$, $H_2O$, and $NO_3^-$ after decomposition.[1-3] Therefore, the bond energy of N1s was analyzed to clarify whether the incompletely degraded RB dye remained on the catalyst surface in the form of physical adsorption. Figure S3 shows that the pure RB dye peaks at 399.4 eV. After piezodegradation for 30 min, the results of $Ti_3C_2T_x$, $Ti_3C_2T_x$-CPTMS, and $Ti_3C_2T_x$-FOTS confirm that the N bonds of RB dye have been chemically decomposed, and $Ti_3C_2T_x$-FOTS show almost 100% degradation.

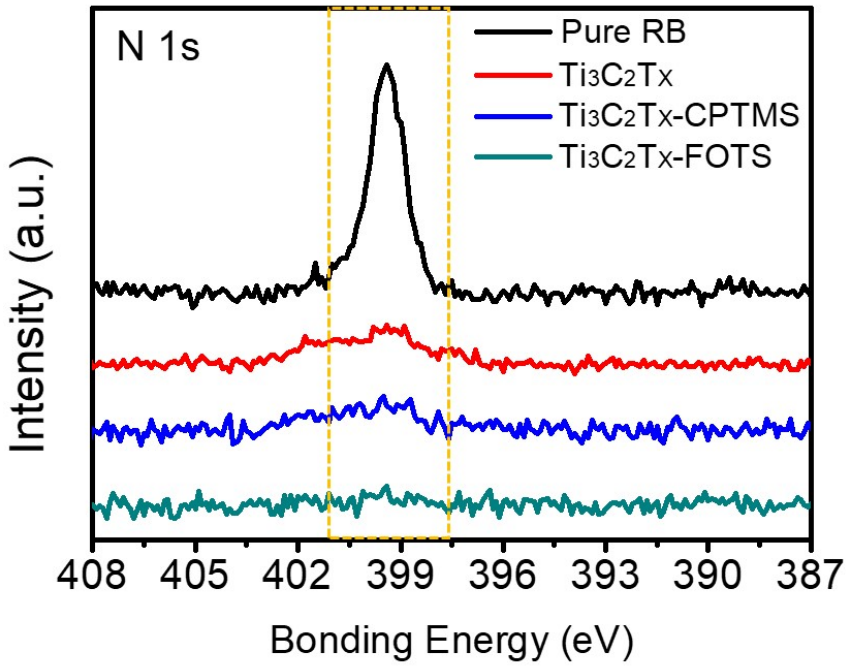


Figure S4. High-resolution XPS spectra of N1s of Pure RB dye, $Ti_3C_2T_x$, $Ti_3C_2T_x$ - CPTMS, and $Ti_3C_2T_x$ - FOTS after the degradation process.

**Supplementary Information of S3**

Table. S1 Comparison of hydrogen production rate and $k_{obs}$ value.

| Catalyst | Type | Driven source | $H_2$ production rate ($\mu mol \cdot g^{-1}h^{-1}$) | Degradation rate constant ($K_{obs}$, $min^{-1}$) | Ref. |
|---|---|---|---|---|---|
| **$Ti_3C_2T_x$-FOTS** | Piezocatalyst | Ultrasonic (300 W) | 900.4 | 0.90 | This study |
| **$MoS_2$** | Piezocatalyst | Ultrasonic (150 W) | 1598.0 | 0.16 | 4 |
| **Quartz/$TiO_2$** | Piezo-photo catalyst | Ultrasonic (200 W) Xe lamp (350 W) | 438.48 | 0.0624 | 5 |
| **$MoS_2$** | Piezocatalyst | Ultrasonic (280 W) | 1250.0 | - | 6 |
| **BNT** | Piezocatalyst | Ultrasonic (110 W) | - | 0.061 | 7 |
| **$PbTiO_3$/CdS** | Piezophoto catalyst | Ultrasonic (300 W) Xe lamp (300 W) | 849.0 | - | 8 |
| **$BaTiO_{3-x}$** | Piezo-photo catalyst | Ultrasonic (100 W) Xe lamp (8 W) | 132.4 | - | 9 |
| **$SrTiO_3$** | Piezo-photo catalyst | Ultrasonic (300 W) Xe lamp (300 W) | 701.2 | - | 10 |
| **BNT@BVO** | Piezocatalyst | Ultrasonic (200 W) Xe lamp (300 W) | - | 0.045 | 11 |
| **$BaTiO_3$** | Piezocatalyst | Ultrasonic (100 W) | - | 0.068 | 12 |

**Supplementary Information of S4**

The following equations show that the sacrificial agent (methanol) has participated in the hydrogen evolution reaction. The piezocatalytic redox reactions are indicated in Eqs. (1)–(5) to explore the generation of molecular species during hydrogen production and wastewater treatment processes.[13-15]

$$MXene \xrightarrow{Piezocatalysis} e^- + h^+ \quad (1)$$

$$H_2O + h^+ \rightarrow {}^{\bullet}OH + H^+ \quad (2)$$

$$CH_3OH + 2h^+ \rightarrow HCHO + 2H^+ \quad (3)$$

$$2H^+ + 2e^- \rightarrow H_2 \quad (4)$$

$$O_2 + e^- \rightarrow {}^{\bullet}O_2^- \quad (5)$$

Eq. (1) reveals piezocatalytic redox reactions in $Ti_3C_2T_x$-FOTS induced by an internal electric field. On sides with a positive piezopotential ($V_p^+$) in $Ti_3C_2T_x$-FOTS, •OH radicals and $H^+$ protons are produced on the active sites of $Ti_3C_2T_x$-FOTS owing to the oxidation of water molecules (Eq. (2)). Additionally, methanol in the solution undergoes oxidation by $Ti_3C_2T_x$-FOTS catalysts, reacting with the holes to generate HCHO with $H^+$ protons, as shown in Eq. (3). Equ. (4) explained that when $H^+$ protons reacted with electrons in $Ti_3C_2T_x$-FOTS with a negative piezopotential ($Vp^-$) to produce the hydrogen gas. Equ. (5) explained that the oxygen reacted with electrons to produce ${}^{\bullet}O_2^-$ radicals. Based on the abovementioned reactions, the piezocatalytic activity can produce •OH and ${}^{\bullet}O_2^-$ radicals, which are the primary species for decomposing dye molecules. Simultaneously, the reaction will generate the $H_2$ gas. Therefore, the $Ti_3C_2T_x$-FOTS exhibited bifunctional activity, consistent with our previous work.[15]

**Supplementary Information of S5**

As shown in Figure S5a-b, the degradation result and hydrogen production rates of $Ti_3C_2T_x$-FOTS demonstrate optimal performance when the functionalizing time exceeds 6 hours. This phenomenon is principally attributed to the saturation of SAMs bonding on the $Ti_3C_2T_x$ MXene surface.

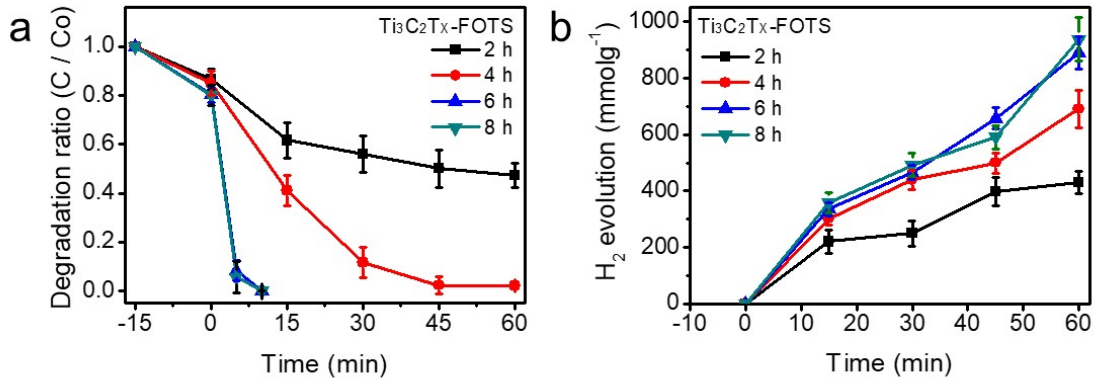


Figure S5. (a) The RB dye degradation performance of $Ti_3C_2T_x$-FOTS and (b) the hydrogen evolution rate of $Ti_3C_2T_x$-FOTS for different functionalizing times.

**Reference**


1. Z.-H. Diao, J.-J. Liu, Y.-X. Hu, L.-J. Kong, D. Jiang and X.-R. Xu, *Sep Purif Technol*, 2017, **184**, 374-383.
2. L. Liang, L. Cheng, Y. Zhang, Q. Wang, Q. Wu, Y. Xue and X. Meng, *Rsc Adv*, 2020, **10**, 28509-28515.
3. Z. He, C. Sun, S. Yang, Y. Ding, H. He and Z. Wang, *J Hazard Mater*, 2009, **162**, 1477-1486.
4. Y. Wang, H. Ma, J. Liu, Z. Zhang, Y. Yu and S. Zuo, *J Colloid Interf Sci*, 2023, **642**, 304-320.
5. M.-C. Lin, S.-N. Lai, K. T. Le and J. M. Wu, *Nano Energy*, 2022, **91**, 106640.
6. Y. Su, L. Zhang, W. Wang, X. Li, Y. Zhang and D. Shao, *J Mater Chem A*, 2018, **6**, 11909-11915.
7. Z. Zhao, L. Wei, S. Li, L. Zhu, Y. Su, Y. Liu, Y. Bu, Y. Lin, W. Liu and Z. Zhang, *J Mater Chem A*, 2020, **8**, 16238-16245.
8. X. Huang, R. Lei, J. Yuan, F. Gao, C. Jiang, W. Feng, J. Zhuang and P. Liu, *Applied Catalysis B: Environmental*, 2021, **282**, 119586.
9. Y. Jiang, C. Y. Toe, S. S. Mofarah, C. Cazorla, S. L. Y. Chang, Y. Yin, Q. Zhang, S. Lim, Y. Yao, R. Tian, Y. Wang, T. Zaman, H. Arandiyan, G. G. Andersson,

J. Scott, P. Koshy, D. Wang and C. C. Sorrell, *Acs Sustain Chem Eng*, 2023, **11**, 3370-3389.
10. Y. Jiang, J. Xie, Z. Lu, J. Hu, A. Hao and Y. Cao, *J Colloid Interf Sci*, 2022, **612**, 111-120.
11. Q. Liu, Q. Hu, D. Zhai, Q. Sun, H. Luo and D. Zhang, *J Mater Chem A*, 2021, **9**, 17841-17854.
12. S. Gao, H. Xing, J. Zhang, Y. Liu, H. Du, Z. Zhu, J. Wang, X. Li, S. Zhang, Y. Yao and L. Ren, *Journal of Materiomics*, 2021, **7**, 1275-1283.
13. J. M. Wu, W. E. Chang, Y. T. Chang and C. K. Chang, *Adv Mater*, 2016, **28**, 3718-3725.
14. Y. J. Chung, C. S. Yang, J. T. Lee, G. H. Wu and J. M. Wu, *Adv Energy Mater*, 2020, **10**.
15. Y. T. Lin, S. N. Lai and J. M. Wu, *Adv Mater*, 2020, **32**, 2002875.